J. Fluid Mech. (2005), *vol.* 535, *pp.* 101–110. © 2005 Cambridge University Press
doi:10.1017/S0022112005004908 Printed in the United Kingdom

Dynamics of suspended particles in eccentrically rotating flows

By EDWIN A. LIM, CARLOS F. M. COIMBRA AND MARCELO H. KOBAYASHI

Department of Mechanical Engineering, University of Hawaii-Manoa, Honolulu, HI 96822, USA
edwinlim@hawaii.edu; coimbra@hawaii.edu; marcelok@hawaii.edu

(Received 5 August 2004 and in revised form 15 April 2005)

The motion of a light particle in an eccentrically rotating cylinder provides a method for verifying stationary history lift force effects at low but non-zero particle Reynolds numbers. We examine the flow in detail using a Lagrangian equation of motion for constant, non-zero-vorticity flows, and we predict a measurable and stationary contribution of history lift effects that can be verified experimentally with current experimental techniques. Because the history lift contribution is relevant only under certain conditions (which are determined in this work), the present flow configuration also allows one to isolate history drag effects under normal gravitation conditions without resorting to the tethered-particle arrangement used in previous works. We formulate and solve the trajectory problem for light particles that attain stable orbital motion, and we propose an experimental concept that makes possible the study of individual contributions of Lagrangian forces to the motion of small particles in viscous flows.

1. Introduction

The history path of a particle moving in a non-uniform viscous flow field is greatly affected by small perturbations over time, i.e. a small force that results only in a minute local change in trajectory may result in a much different overall particle trajectory far downstream from the local position. It is therefore of interest to study equations of motion that can describe particle–flow interactions as accurately as possible. The equation proposed in Coimbra & Kobayashi (2002) is used in this work to determine the effect that the history lift force has on the motion of a particle in an eccentrically rotating flow. The stationary and stable orbital motion described by the particle is used to determine whether or not history lift effects can be measured with the available temporal and spatial resolutions of conventional experimental methods (Coimbra *et al.* 2004). Hence, this work provides not only a complete formulation for the dynamics of suspended particles in eccentrically rotating flows, but also relevant criteria for the design of experiments that can potentially validate each one of the viscous forces that determine particle trajectories in non-uniform, time-dependent flows.

Because of its importance in both natural and engineered flows, the motion of a single small sphere in a viscous flow has been studied extensively for both infinitesimal (see e.g. Boussinesq 1885; Basset 1888; Hjelmfelt & Mockros 1966; Chao 1968; Reeks & McKee 1984; Mei, Adrian & Hanratty 1991; Chaoui & Feuillebois 2003) and finite particle Reynolds numbers (see e.g. McLaughlin 1991; Mei &

https://doi.org/10.1017/S0022112005004908 Published online by Cambridge University Press

Adrian 1992; Lovalenti & Brady 1993; Chang & Maxey 1994; Kim, Elghobashi & Sirignano 1998). The transient, infinitesimal Reynolds number (Stokes flow), particle response in a uniform but time-dependent background flow was solved exactly by Coimbra & Rangel (1998). The transient and stationary behaviour of particle motion in harmonically forced Stokes flow is discussed in detail in Coimbra & Rangel (2001) and in the references therein. Stationary one-directional history effects have been recently verified experimentally by Coimbra *et al.* (2004) for high Strouhal number, low particle Reynolds number flows, thus validating the classical Basset kernel of the history force in Tchen's equation (Tchen 1947) for a wide range of the relevant parameters (Reynolds and Strouhal numbers), and for both heavy and light particles. Coimbra & Kobayashi (2002) proposed the incorporation of steady Saffman and history inertial lift effects into an equation of motion that is relevant to constant-vorticity flows (Saffman 1965). In that work, Coimbra & Kobayashi analysed the special case of uniform and steady rotational flows, which represents one of the simplest possible shear flows where lift effects can be observed and quantified without the presence of solid walls. In particular, the rotating cylinder case provides a steady-state equilibrium position for light particles that can be verified experimentally. The equation proposed in Coimbra & Kobayashi (2002) was compared with the classic Maxey–Riley equation (Maxey & Riley 1983), which was derived for the limit of infinitesimal particle Reynolds numbers and therefore does not take into account inertial lift effects. Some key differences are found by including lift effects, including a shift in the position of the equilibrium points to a different quadrant in respect to the axis of the rotating cylinder and the gravitational vector.

In the present work, we focus our attention on the less studied history lift force and propose an experiment that can ascertain the validity of the history lift functional form as a half-derivative of the steady Saffman lift (Coimbra & Kobayashi 2002). Although a formal derivation of the history lift force in closed form requires a laborious perturbation analysis for the first asymptotic inertial time-dependent terms, the arguments and the scaling analysis used in Coimbra & Kobayashi (2002) indicate that the kernel of the history lift force is in fact a half-derivative of the steady Saffman lift force. This argument is analogous to the Basset history drag being a half-derivative of the steady Stokes drag, and makes use of the fact that the Saffman lift force has the same form as the Stokes drag when the migration velocity replaces the slip velocity. The Basset-like form of the kernel of the history term is in agreement with the asymptotic behaviour found by Asmolov & McLaughlin (1999) for high-frequency flows. In order to produce a stationary history lift effect that is measurable over time, we introduce a time-dependent, periodic forcing that does not, however, affect the constant vorticity of the background flow. The proposed eccentrically rotating configuration is a straightforward modification of the horizontally rotating cylinder that generates history drag and lift effects in a stationary way. Thus, the eccentric cylinder configuration yields results that are conducive to experimental verification, and does not affect the validity of the equation in use.

2. Eccentric rotating cylinder model

We consider a rotating cylinder filled with a viscous fluid, oriented such that its axis is in a plane perpendicular to the gravitational acceleration. The axis of the cylinder undergoes circular motion about the rotating axis (see figure 1). The centre of mass of the cylinder thus describes a circle while maintaining its horizontal orientation in respect to gravity.

https://doi.org/10.1017/S0022112005004908 Published online by Cambridge University Press

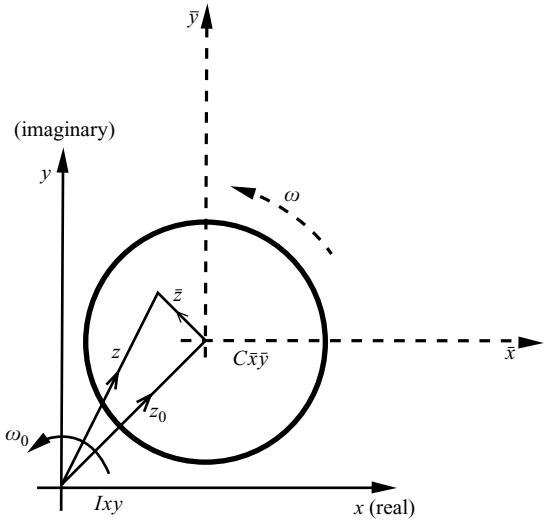


FIGURE 1. Reference frames used in the computation: Ixy is the inertial reference frame with origin at the centre of the eccentric and $C\bar{x}\bar{y}$ is the non-inertial frame attached to the centre of the cylinder.

Because the flow field and the gravitational acceleration are co-planar, a spherical particle introduced into the fluid will have a trajectory that is similarly constrained. This observation allows the problem to be modelled in two dimensions. We take advantage of the commutative algebra of complex numbers by using the identification $\mathbb{C} \equiv \mathbb{R}^2$. Note that we adopt the convention of using upper-case symbols to designate dimensional quantities and the respective lower-case symbols to designate dimensionless quantities. Exceptions to this convention should be obvious enough to avoid any confusion ($Re_p \equiv$ Reynolds number, $Sl \equiv$ Strouhal number, etc.).

Also, given the nature of the motion of the eccentric cylinder, it is appropriate to look at the system using two reference frames, which we will refer to as the cylinder reference frame and the inertial reference frame. The cylinder, or non-inertial, reference frame, $C\bar{x}\bar{y}$, is attached to the centre of the rotating cylinder, with the positive y-(imaginary) axis pointing in the direction opposite to gravity. The inertial reference frame, Ixy, is centred on the fixed point about which the cylinder is translating. The origin of $C\bar{x}\bar{y}$ is then moving around the origin of Ixy with a constant radius of R_0 and a constant angular velocity of Ω_0. Note that Ixy is oriented in the same way as $C\bar{x}\bar{y}$ at all times, with the y-axis pointing away from gravity. So, in the inertial frame, the centre of the cylinder has the position vector $\boldsymbol{Z}_0(T) = \boldsymbol{R}_0 \mathrm{e}^{\mathrm{i}\omega_0 T}$ at a given time T. For simplicity, we assume that position vector to be at zero radian at $T = 0$, i.e. $\boldsymbol{Z}_0(T = 0) = \boldsymbol{R}_0$.

If the position vectors in the inertia reference frame and the cylinder reference frame are denoted by $\boldsymbol{Z}$ and $\bar{\boldsymbol{Z}}$, respectively, then we can move from one reference frame to the other with the (time-dependent) transformation

$$\boldsymbol{Z} = \bar{\boldsymbol{Z}} + \boldsymbol{Z}_0(T). \tag{2.1}$$

3. Lagrangian equation of particle motion in uniform vorticity flows

For a constant-gradient flow $\boldsymbol{U}(\boldsymbol{X}, T)$ with constant vorticity ($\mathscr{Z} = \nabla \times \boldsymbol{U} = \text{constant}$), the Laplacian is null ($\nabla^2 \boldsymbol{U} = 0$), and the Lagrangian equation of

https://doi.org/10.1017/S0022112005004908 Published online by Cambridge University Press

motion for a particle in the low shear Reynolds number ($Re_s \ll 1$) regime (Coimbra & Kobayashi 2002) is

$$m_p \mathscr{D}(\boldsymbol{V}) = m_f \frac{\mathrm{D}\boldsymbol{U}}{\mathrm{D}T} - \frac{m_f}{2}\left[\mathscr{D}(\boldsymbol{V}) - \frac{\mathrm{D}\boldsymbol{U}}{\mathrm{D}T}\right] - \frac{a\Lambda_S}{\nu^{1/2}}\mathscr{D}^{1/2}(\boldsymbol{W}) - \Lambda_S(\boldsymbol{W}) + C_S a^2 \left(\frac{\mu\rho_f}{|\mathscr{Z}|}\right)^{1/2} \mathscr{Z} \times \boldsymbol{W} + C_S a^3 \rho_f \left(\frac{1}{|\mathscr{Z}|}\right)^{1/2} \mathscr{D}^{1/2}(\mathscr{Z} \times \boldsymbol{W}) + (m_p - m_f)\boldsymbol{G}. \quad (3.1)$$

The symbol $\boldsymbol{V}$ represents the absolute velocity of the particle and $\boldsymbol{W}$ is the particle velocity relative to the fluid. Other relevant variables and parameters include: particle radius, a; kinematic and dynamic viscosities, ν and μ; the masses of the particle and displaced fluid, m_p and m_f, and the corresponding densities, ρ_p and ρ_f. The symbol $\mathscr{D}$ is the generalized differential operator in dimensional time T, which is formally defined for regular functions as

$$\mathscr{D}^q \boldsymbol{f} = \begin{cases} \dfrac{1}{\Gamma(-q)} \displaystyle\int_{-\infty}^{T} (T-\sigma)^{-q-1} \boldsymbol{f}(\sigma)\mathrm{d}\sigma, & q < 0 \\ \dfrac{1}{\Gamma(p-q)} \dfrac{\mathrm{d}^p}{\mathrm{d}T^p} \displaystyle\int_{-\infty}^{T} (T-\sigma)^{p-q-1} \boldsymbol{f}(\sigma)\mathrm{d}\sigma, & q \geqslant 0, \end{cases} \quad (3.2)$$

where $\Gamma(s)$ is the Gamma (generalized factorial) function of s, and $p-1 \leqslant q < p$ with $p = 1, 2, \ldots$. Thus, $\mathscr{D} \equiv \mathrm{d}/\mathrm{d}T$, $\mathscr{D}^2 \equiv \mathrm{d}^2/\mathrm{d}T^2$, etc. Then, $\mathscr{D}^{1/2} \equiv \mathrm{d}^{1/2}/\mathrm{d}T^{1/2}$ is called a half-order derivative or semi-derivative, and by (3.2) with $q = 1/2$ and $p = 1$, is

$$\mathscr{D}^{1/2} \boldsymbol{f} = \frac{1}{\sqrt{\pi}} \frac{\mathrm{d}}{\mathrm{d}T} \int_{-\infty}^{T} \frac{\boldsymbol{f}(\sigma)}{\sqrt{(T-\sigma)}}\,\mathrm{d}\sigma = \frac{1}{\sqrt{\pi}} \int_{-\infty}^{T} \frac{\mathrm{d}\boldsymbol{f}(\sigma)}{\mathrm{d}\sigma} \frac{1}{\sqrt{(T-\sigma)}}\,\mathrm{d}\sigma. \quad (3.3)$$

Note that $\mathscr{Z} = \nabla \times \boldsymbol{U}$ here is vorticity, to be distinguished from $\boldsymbol{Z}$, the position vector in the complex plane. The symbol $\boldsymbol{X}$ stands for the general position vector in $\mathbb{R}^3$.

Equation (3.1) is simply Newton's Second Law with all the fluid force terms on the right-hand side. The so-called pressure term is represented by the two $\mathrm{D}\boldsymbol{U}/\mathrm{D}T$ terms. The second term containing the square brackets is the *added mass force* (see e.g. Lamb 1945). The next two terms represent the viscous drag forces: history drag (with the semi-derivative) and Stokes drag, with $\Lambda_S = 6\pi\mu a$ as the Stokes drag coefficient. These are followed by the lift effects: history lift (again, with the semi-derivative) and Saffman lift (Saffman 1965). The Saffman lift coefficient C_S has a numerical value of 6.46 in the linear regime ($Re_s < 1$). Gravity effects are included in the buoyancy-weight term on the right-hand side of (3.1).

Equation (3.1) was proposed by Coimbra & Kobayashi (2002) after a detailed scaling analysis that justifies its use for uniform-vorticity flows in the range $Re_p \sim Re_s < 1$. Note that (2.9) in Coimbra & Kobayashi (2002) contains a typographical error in the dimensional form of the history lift force. The correct expression is shown in (3.1) above, as well as in previous publications (Ramirez *et al.* 2003). The inclusion of inertial lift effects is necessary when departing from the infinitesimal Re_p limit in uniform-vorticity flows, even though the absolute value of the lift force is typically much smaller than the steady and history drag forces or the gravitational contribution (for a detailed description of the evolution of forces in time, and experimental verification of the effectiveness of Lagrangian equations in unsteady flows, see Ramirez *et al.*, 2003; Candelier, Angilella & Souhar 2004; and Coimbra *et al.* 2004). The rationale for including the history lift force in (3.1) follows from scaling arguments that take into consideration the unsteady effect of a linearized Saffman-like point force

https://doi.org/10.1017/S0022112005004908 Published online by Cambridge University Press

on the motion of the particle (Coimbra & Kobayashi 2002). The scaling analysis leads to a Basset-like kernel for the history lift force that corroborates the high-frequency limit of the asymptotic-numerical analysis of Asmolov & McLaughlin (1999). The Basset kernel implies an inverse-square-root dependence on the rotating frequency for the total lift force in the range of parameters under study in the present work ($Re_p \sim Re_s < 1$).

3.1. *Non-dimensionalization*

We non-dimensionalize (3.1) using the particle radius for length, and a characteristic time scale τ_p for time. To aid in the non-dimensionalization process, it is useful to define the mass (or density) ratio $\alpha = m_f/m_p = \rho_f/\rho_p$. With that, a characteristic time scale can be written as $\tau_p = 2a^2/(9\nu\alpha\gamma)$ where $\gamma = 2/(2+\alpha)$. The non-dimensional form of (3.1) is thus

$$\mathscr{D}(\boldsymbol{v}) = 3\hbar\frac{\mathrm{D}\boldsymbol{u}}{\mathrm{D}t} - \boldsymbol{w} - 3\hbar^{1/2}\mathscr{D}^{1/2}(\boldsymbol{w}) + C_L(\boldsymbol{\zeta}\times\boldsymbol{w}) + 3C_L\hbar^{1/2}\mathscr{D}^{1/2}(\boldsymbol{\zeta}\times\boldsymbol{w}) + \boldsymbol{g}, \quad (3.4)$$

with the variables in lower case representing the dimensionless versions of their respective counterparts. This dimensionless form has the advantage that there are only two parameters, $\hbar = \alpha/(2+\alpha)$ and C_L, the lift coefficient, which is defined as

$$C_L \equiv \frac{C_S}{2\pi}\sqrt{\frac{\hbar}{|\boldsymbol{\zeta}|}}. \quad (3.5)$$

The dimensionless gravitational effect, $\boldsymbol{g}$, has the magnitude of $Re_{p,\tau}/(9\hbar)$ and acts in the direction of gravity, or

$$\boldsymbol{g} = -\frac{Re_{p,\tau}}{9\hbar}\hat{\boldsymbol{j}}, \quad (3.6)$$

where $Re_{p,\tau}$ is the terminal particle Reynolds number, given by $Re_{p,\tau} = aV_\tau/\nu$. In terms of the quantities defined above, the terminal velocity of a sphere falling under gravity in an otherwise quiescent fluid is $V_\tau = (1-\alpha)\gamma\tau_p G_c$, with $G_c = 9.81\,\mathrm{m\,s^{-1}}$ as the gravitational constant.

3.2. *Transformation into the complex domain*

To transform (3.4) to the complex domain, we use the following identities: $\boldsymbol{v} = \mathscr{D}z = \mathscr{D}\bar{z} + \mathrm{i}\omega_0 z_0$; $\boldsymbol{u} = \mathrm{i}\omega\bar{z} + \mathrm{i}\omega_0 z_0$; $\boldsymbol{w} = \boldsymbol{v} - \boldsymbol{u} = \mathscr{D}\bar{z} - \mathrm{i}\omega\bar{z}$; $\boldsymbol{\zeta}\times\bar{z} = 2\mathrm{i}\omega\bar{z}$; $\boldsymbol{\zeta}\times\boldsymbol{u} = -2\omega^2\bar{z} - 2\omega\omega_0 z_0$; $\boldsymbol{\zeta}\times\boldsymbol{v} = 2\omega(\mathrm{i}\mathscr{D}\bar{z} - \omega_0 z_0)$; $\boldsymbol{\zeta}\times\boldsymbol{w} = 2\omega(\mathrm{i}\mathscr{D}\bar{z} + \omega\bar{z})$; $\mathrm{D}u/\mathrm{D}t = -\omega_0^2 z_0 - \omega^2\bar{z}$; and $\mathscr{D}^2 z_0 = -\omega_0^2 z_0$. For our case of two-dimensional flow, the vorticity cross-product is treated as an operator such that $\boldsymbol{\zeta}\times \equiv 2\mathrm{i}\omega$. With the above identities, equation (3.4) is represented in the complex domain by the apparent motion $\bar{z}(t)$:

$$\begin{aligned}\mathscr{D}^2\bar{z} + 3\hbar^{1/2}(1-2\mathrm{i}C_L\omega)\mathscr{D}^{3/2}\bar{z} + (1-2\mathrm{i}C_L\omega)\mathscr{D}\bar{z} - 3\mathrm{i}\hbar^{1/2}\omega(1-2\mathrm{i}C_L\omega)\mathscr{D}^{1/2}\bar{z} \\ + [3\hbar\omega^2 - \mathrm{i}\omega(1-2\mathrm{i}C_L\omega)]\bar{z} = (1-3\hbar)\omega_0^2 z_0 + \boldsymbol{g}. \quad (3.7)\end{aligned}$$

Equation (3.7) is a linear non-homogeneous fractional differential equation with constant coefficients. Recall that $\bar{z}(t)$ is the position vector of the particle with respect to the cylinder frame and $z_0(t)$ (known for all time) is the position vector of the cylinder frame with respect to the inertial frame.

Equation (3.7) can be written in a more compact form as

$$\mathscr{D}^2\bar{z} + (1-2\mathrm{i}C_L\omega)\left(1 + 3\hbar^{1/2}\mathscr{D}^{1/2}\right)(\mathscr{D}\bar{z} - \mathrm{i}\omega\bar{z}) + 3\hbar\omega^2\bar{z} = (1-3\hbar)\omega_0^2 z_0 + \boldsymbol{g}. \quad (3.8)$$

The above form has the advantage of showing explicitly the drag and lift forces as well as the 'normal' and history components of those forces. The second term

https://doi.org/10.1017/S0022112005004908 Published online by Cambridge University Press

of the left-hand side is associated with the drag and lift effects. The terms in the first parentheses represent drag and lift components with drag being unity and lift as $-2\mathrm{i}C_L\omega$. The terms in the second parentheses indicate the 'normal' and history components, with the normal component being unity and the history component represented by the operator $3\hbar^{1/2}\mathscr{D}^{1/2}$. The remaining two terms on the left-hand side relate to the pressure term ($3\hbar\omega^2\bar{z}$) and to the acceleration of the particle ($\mathscr{D}^2\bar{z}$).

3.3. *Superposition of solutions*

Since (3.8) is linear, we can solve it in two stages by separating it into two equations

$$\mathscr{D}^2 H\bar{z}_g + (1-2\mathrm{i}C_L\omega)\big(1+3\hbar^{1/2}\mathscr{D}^{1/2}\big)(\mathscr{D}H\bar{z}_g - \mathrm{i}\omega H\bar{z}_g) + 3\hbar\omega^2 H\bar{z}_g = +H\boldsymbol{g} \tag{3.9}$$

and

$$\mathscr{D}^2\bar{z}_0 + (1-2\mathrm{i}C_L\omega)\big(1+3\hbar^{1/2}\mathscr{D}^{1/2}\big)(\mathscr{D}\bar{z}_0 - \mathrm{i}\omega\bar{z}_0) + 3\hbar\omega^2\bar{z}_0 = (1-3\hbar)\omega_0^2 z_0. \tag{3.10}$$

The first equation gives the response of the particle to a step function H with amplitude $\boldsymbol{g}$ and null initial conditions $\bar{z}_g(0) = \mathscr{D}\bar{z}_g|_{t=0} = 0$. That is, the particle, fixed to $\bar{z}=0$ for $t\leqslant 0^-$, is freed and allowed to respond to gravity from $t=0^+$. This gives us a known (null) history at $t=0^+$. Note that more general initial conditions can be handled by adjoining the corresponding term in the equation. Since this is not relevant for our purposes, we consider only the null initial conditions for simplicity.

The second equation represents the particle response to the translation of the cylinder about the fixed point. We will refer to this contribution to the particle motion as the frequency response.

The solution to (3.8) is then the combination of the solutions of (3.9) and (3.10): $\bar{z}=\bar{z}_g+\bar{z}_0$. The solution of (3.9) can be found in Coimbra & Kobayashi (2002) and will not be repeated here. This leaves us the task of solving (3.10) for $\bar{z}_0$.

3.4. *Frequency response*

As the homogeneous solution to (3.10) is exactly the same as the homogeneous solution to (3.9), all that is needed now is the particular solution to (3.10), which we will indicate with $\bar{z}_{0,p}$. The general solution of the apparent motion, $\bar{z}=\bar{z}_g+\bar{z}_0$, can be represented equivalently by $\bar{z}=\bar{z}_g+\bar{z}_{0,p}$.

Recalling that $z_0 = r_0\mathrm{e}^{\mathrm{i}\omega_0 t}$, we therefore seek the particular solution $\bar{z}_{0,p} = \boldsymbol{Z}_n r_0\mathrm{e}^{\mathrm{i}\omega_0 t}$ using the method of undetermined coefficients as is appropriate for a constant-coefficient, fractional differential equation. Substituting this expression in equation (3.10) and solving for $\boldsymbol{Z}_n$ gives

$$\boldsymbol{Z}_n = \frac{(1-3\hbar)\delta^2}{-\delta^2+3\hbar+\mathrm{i}(9\hbar/Re_s)(1-2\mathrm{i}C_L Re_s/9\hbar)\big(1+\mathrm{e}^{\mathrm{i}\pi/4}\sqrt{\delta Re_s}\big)(\delta-1)} \tag{3.11}$$

where $\delta=\omega_0/\omega$ is the ratio of the frequencies, and Re_s is the characteristic shear Reynolds number defined as $Re_s = a^2\Omega/\nu = 9\hbar\omega$. Note that Re_s is constant for a uniform-vorticity flow. The denominator originates from the left-hand side of (3.10), and allows us to trace each term to its parent force. The term $-\delta^2$ is due to the acceleration of the particle, $3\hbar$ is due to the pressure term, and the large factored term represents the drag and lift forces: $1-2\mathrm{i}C_L Re_s/(9\hbar)$ for drag and lift, and $1+\mathrm{e}^{\mathrm{i}\pi/4}\sqrt{\delta Re_s}$ the normal and history components of these forces.

To get the particle trajectory in the inertial reference frame, we employ the dimensionless equivalent of (2.1), giving us

$$z = \bar{z}_g + \boldsymbol{Z}_n r_0\mathrm{e}^{\mathrm{i}\omega_0 t} + r_0\mathrm{e}^{\mathrm{i}\omega_0 t}. \tag{3.12}$$

https://doi.org/10.1017/S0022112005004908 Published online by Cambridge University Press

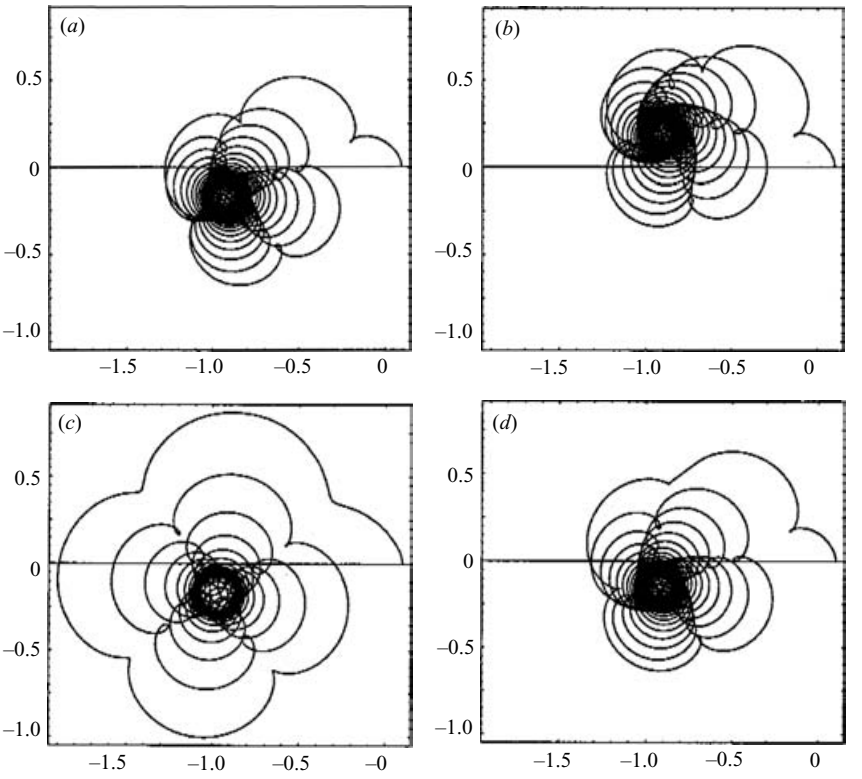


FIGURE 2. Particle trajectories $z(t)$ as seen by an observer in the inertial reference frame Ixy: (*a*) the trajectory as described by (3.7); (*b*) the absence of lift effects; (*c*) missing both history drag and history lift; and (*d*) (3.7) without history lift. The parameters for the flow are: $Re_{p,\tau} = Re_s = 0.7$, $\alpha = 2$ (denser fluid), $r_0 = 0.1$ and $\delta = 5$. Lengths are normalized by particle radius.

3.5. *Reduction to the simple rotating cylinder*

Together with (3.11), it is noted that in two special cases, the problem reduces to that of the gravitational response of a particle in a simple rotating cylinder, as described in Coimbra & Kobayashi (2002). The first case is when the eccentric radius vanishes, $r_0 = 0$, and with it the two last terms of (3.12). The second case is when both the cylinder rotation and translation frequencies coincide, $\omega_0/\omega = \delta = 1$. In this case the fluid is effectively rotating about the inertia fixed point as well as the centre of the cylinder, and the particle trajectory should be as if it were in a simple virtual rotating cylinder centred on the inertia fixed point. This is confirmed in equation (3.12) for $\boldsymbol{Z}_n|_{\delta=1} = -1$, where the two last terms cancel each other's effects.

4. Results

Figure 2 shows the particle paths predicted by different equations of motion. The significantly different trajectories underscore the importance of finding the correct equation of motion. Compared to (3.7), the difference in particle path calculated using only Stokes drag (and pressure) is obvious and striking. Figure 2(*b*) represents a trajectory that would have been predicted using the equation proposed in Maxey & Riley (1983), since the equation neglects lift effect in a flow with uniform shear. Note

https://doi.org/10.1017/S0022112005004908 Published online by Cambridge University Press

that the long-time quasi-steady orbit of the particle is above the horizontal axis of the fixed point when there is no lift. Figure 2(*c*) shows the importance of history effects, reaffirming the findings of Candelier *et al.* (2004). With lift force but no history lift effect, figure 2(*d*) shows a particle path that is closer to that of figure 2(*a*). However, there are still differences in the particle paths which will be explored in a little more detail below.

4.1. *The history lift difference*

Although, as can be seen in figures 2(*a*) and 2(*d*), the particle paths with and without history lift are clearly different, it is not immediately clear how to quantify the difference in a useful manner. What is desired is an appropriate quantification that is able to capture the history effect and, preferably, conducive to experimental verification. To that end, we look at the effect of history lift on the quasi-steady (long-time) trajectory of the particle.

Rewriting (3.12) as

$$z = \bar{z}_g + (\boldsymbol{Z}_n + 1) r_0 \mathrm{e}^{\mathrm{i}\omega_0 t}, \tag{4.1}$$

it becomes clear that as $t \to \infty$, $\bar{z}_g$ converges to a constant (for a light particle, as in Coimbra & Kobayashi 2002), and z then describes a circular orbit of radius $|\boldsymbol{Z}_n + 1|\, r_0$ about this constant $\bar{z}_g(t \to \infty)$. Since history forces (both lift and drag) vanish for a particle in equilibrium, $\bar{z}_g(t \to \infty)$ is the same whether history lift is considered or not. It then follows that in order to see the effect of history lift on the long-time quasi-steady particle path, we only need to look at the effect of history lift on $(\boldsymbol{Z}_n + 1)$.

An approach for quantifying the effect of history lift on $(\boldsymbol{Z}_n + 1)$ is to look at the difference in stable orbital radii (normalized with the eccentric radius) $|\boldsymbol{Z}_n + 1|$ in the presence and absence of the history lift term. For the results from experimental verification to be unambiguous, it is desired that the difference between with and without history lift

$$\Delta_{\mathrm{HL}} = |\boldsymbol{Z}_n + 1|_{\text{no history lift}} - |\boldsymbol{Z}_n + 1| \tag{4.2}$$

be at least one order of magnitude larger than the experimental uncertainty. In order to establish the conditions for an experiment we first realize that although Δ_{HL} is a function of only three dimensionless parameters (Re_s, $\hbar$ and δ), the dependence of Δ_{HL} on these three parameters is not trivial. The experiments must also conform to the three constraints $Re_p < 1$, $Re_p \leqslant \sqrt{Re_s}$, and $\alpha > 1$ (or $\hbar > 1/3$) that are required for the validity of the equation and for achieving a stable orbit. We can take advantage of the constraints by noting that, in general, larger Re_s, α and δ produce larger Δ_{HL}. Also, there exist values of $\delta \sim 1$ that yield the large Δ_{HL} that we seek (figure 3).

An example of physical parameters that match favourable conditions for an experiment makes use of a fluid of viscosity similar to castor oil ($\mu = 1.8 \times 10^{-3}\ \mathrm{m^2\ s^{-1}}$, $\rho_f = 960\ \mathrm{kg\ m^{-3}}$) and a hollow polypropylene ball (radius $a = 5\ \mathrm{mm}$, $\rho_p = 440\ \mathrm{kg\ m^{-3}}$). A rotation frequency within the constraints of Re_s would be of the order of $\Omega = 600$ r.p.m. Translation frequency of the cylinder can be selected by taking advantage of the maximum at $\delta = 1.1$, so $\Omega_0 = 660$ r.p.m. Since Δ_{HL} is normalized with respect to the eccentric translation radius r_0, we can select a large eccentricity, say 1.5 mm or $r_0 = 0.3$. With these parameters, equations (4.2) and (3.11) predict an orbital radius difference of 0.17 mm, the orbital radii with and without history lift being 1.46 mm and 1.63 mm respectively. The relevant parameters for this example are $Re_s = 0.867$, $\alpha = 2.18$ and $\delta = 1.1$.

https://doi.org/10.1017/S0022112005004908 Published online by Cambridge University Press

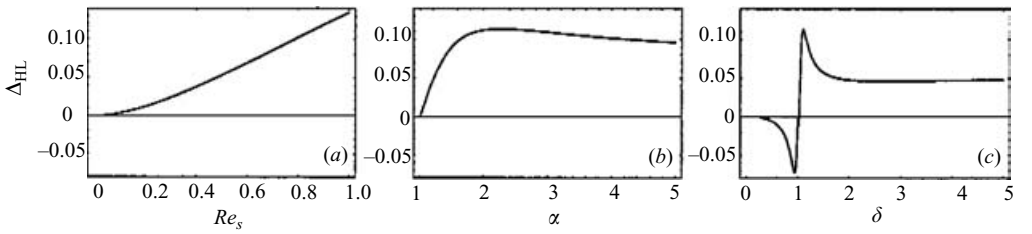


FIGURE 3. Difference in steady orbital radii with and without history lift effect. These plots show the effects on the difference in radii when (*a*) Re_s, (*b*) α ($\hbar$) and (*c*) δ are varied about the example experimental parameters of $Re_s = 0.867$, $\alpha = 2.18$ and $\delta = 1.1$. The Δ_{HL} axis represents dimensionless values.

5. Conclusions

We studied the motion of a light particle in an eccentrically rotating cylinder in order to examine conditions for which history lift effects become relevant in a stationary sense. The importance of lift and drag forces is illustrated through the exact solution of the proposed equation of motion. We characterize the range of parameters for which stationary history lift effects are relevant and measurable. The flow under study presents a suitable candidate for experimental validation of Lagrangian forces that can be performed with instrumentation currently available (Coimbra *et al.* 2004).

C.F.M.C. and E.A.L. wish to acknowledge the funding provided by the American Chemical Society for partial support of this research. M.H.K. is partially supported by the Portuguese FCT under grant POCTI/36271/EME/2000.

REFERENCES

ASMOLOV, E. S. & MCLAUGHLIN, J. B. 1999 The inertial lift on an oscillating sphere in a linear shear flow. *Intl J. Multiphase Flow* **25**, 739–751.

BASSET, A. B. 1888 On the motion of a sphere in a viscous liquid. *Phil. Trans. R. Soc. Lond.* A **179**, 43–63.

BOUSSINESQ, J. 1885 Sur la résistance qu'oppose un liquide indéfini en repos, sans pesanteur, au mouvement varié d'une sphère solide qu'il mouille sur toute sa surface, quand les vitesses restent bien continues et assez faibles pour que leurs carrés et produits soient négligeables. *C. R. Acad. Sci. Paris* **100**, 935–937.

CANDELIER, F., ANGILELLA, J. & SOUHAR, M. 2004 On the effect of the Boussinesq-Basset force on the radial migration of a Stokes particle in a vortex. *Phys. Fluids* **16**, 1765–1776.

CHANG, E. J. & MAXEY, M. R. 1994 Unsteady flow about a sphere at low to moderate Reynolds number. Part 1. Oscillatory motion. *J. Fluid Mech.* **277**, 347–379.

CHAO, B. T. 1968 Turbulent transport behavior of small particles in dilute suspension. *Österreichisches Ing. Arch.* **18**, 7–21.

CHAOUI, M. & FEUILLEBOIS, F. 2003 Creeping flow around a sphere in a shear flow close to a wall. *Q. J. Mech. Appl. Maths* **56**, 381–410.

COIMBRA, C. F. M. & KOBAYASHI, M. H. 2002 On the viscous motion of a small particle in a rotating cylinder. *J. Fluid Mech.* **469**, 257–286.

COIMBRA, C. F. M., L'ESPERANCE, D., LAMBERT, R. A., TROLINGER, J. D. & RANGEL, R. H. 2004 An experimental study on stationary history effects on high-frequency Stokes flows. *J. Fluid Mech.* **504**, 353–363.

COIMBRA, C. F. M. & RANGEL, R. H. 1998 General solution of the particle momentum equation in unsteady Stokes flow. *J. Fluid Mech.* **370**, 53–72.

https://doi.org/10.1017/S0022112005004908 Published online by Cambridge University Press

Coimbra, C. F. M. & Rangel, R. H. 2001 Spherical particle motion in harmonic Stokes flows. *AIAA J.* **39**, 1673–1682.

Hjelmfelt, A. T. & Mockros, L. F. 1966 Motion of discrete particles in turbulent fluid. *Appl. Sci. Res.* **16**, 148–161.

Kim, I., Elghobashi, S. E. & Sirignano, W. A. 1998 On the equation of motion for spherical-particle motion: effects of Reynolds and acceleration numbers. *J. Fluid Mech.* **367**, 221–253.

Lamb, S. H. 1945 *Hydrodynamics*, 6th Edn. Dover.

Lovalenti, P. M. & Brady, J. F. 1993 The hydrodynamic force on a rigid particle undergoing arbitrary time-dependent motion at small Reynolds number. *J. Fluid Mech.* **256**, 561–605.

Maxey, M. R. & Riley, J. J. 1983 Equation of motion for a small rigid sphere in a non-uniform flow. *Phys. Fluids* **26**, 883–888.

McLaughlin, J. B. 1991 Inertial migration of a small sphere in linear shear flows. *J. Fluid Mech.* **224**, 261–274.

Mei, R. W. & Adrian, R. J. 1992 Flow past a sphere with an oscillation in the free-stream velocity and unsteady drag at finite Reynolds number. *J. Fluid Mech.* **237**, 323–341.

Mei, R. W., Adrian, R. J. & Hanratty, T. J. 1991 Particle dispersion in isotropic turbulence under Stokes drag and Basset force with gravitational settling. *J. Fluid Mech.* **225**, 481–495.

Ramirez, L. E. S., Lim, E. A., Coimbra, C. F. M. & Kobayashi, M. H. 2003 On the dynamics of a spherical scaffold in rotating wall bioreactors. *Biotech. Bioengng* **84**, 382–389.

Reeks, M. W. & McKee, S. 1984 The dispersive effects of Basset history forces on particle motion in a turbulent flow. *Phys. Fluids* **27**, 1573–1582.

Saffman, P. G. 1965 The lift on a small sphere in a slow shear flow. *J. Fluid Mech.* **22**, 385–400.

Tchen, C. M. 1947 Mean value and correlation problems connected with the motion of small particles suspended in a turbulent fluid. Doctoral dissertation, Delft University, The Hague.

https://doi.org/10.1017/S0022112005004908 Published online by Cambridge University Press